Demonstration of complementarity between path information and interference with thermal light

Ling-Yu Dou,[1] Yaron Silberberg,[2] and Xin-Bing Song[1,2,*]
[1]*School of Physics, Beijing Institute of Technology, Beijing 100081, China*
[2]*Department of Physics of Complex Systems, Weizmann Institute of Science, Rehovot 76100, Israel*

(Received 4 October 2018; published 15 January 2019)

We report an experimental demonstration of complementarity between path information and interference in second-order correlation with thermal light. The key apparatus is a Sagnac interferometer in which an off-axis slit is inserted. Two orthogonal thermal light beams travel through the slit clockwise and anticlockwise in the interferometer. The second-order interference fringes vanish when the path information is acquired. The interference fringes are revived when the path information is effaced.

DOI: 10.1103/PhysRevA.99.013825

Wave-particle duality has puzzled physicists since the early days of quantum mechanics. Bohr and others discussed various gedanken experiments, such as Young's double-slit experiment with a recoiling slit [1], to demonstrate the principle of complementarity: how precise "which way" knowledge eliminates wave interference. Although it is prohibited to observe the wave and particle behaviors simultaneously, more and more efforts have been concentrated on complementarity theoretically [2–7] and experimentally [8–16]. At the beginning, single particles, such as single photons, ions, or atoms, were used to examine complementarity. However, one of the biggest imperfections is that auxiliary interaction directly disturbs the only particle when its path information is measured. To circumvent this imperfection, multiparticle schemes were then proposed in a nonlocal way. In 1994, Jaeger *et al.* theoretically analyzed complementarity between distinguishability of the path and the visibility of the interference pattern for a single-particle and two-particle schemes [17]. Later, experimental demonstration between one- and two-photon interference in a Young's experiment with entangled photons via spontaneous parametric down-conversion was reported by Abouraddy *et al.* [18]. In many cases, the quantum state of the light source is prepared and modulated in a delicate way to transfer the interference between one- and two-photon coherence. In recent years, for example, a scheme of a double-slit experiment using two entangled photons created via spontaneous parametric down-conversion was investigated to observe interference of the signal photon despite the fact that the signal photon was located in one of the slits due to its entanglement with the idler photon [19–21]. The explanation of this puzzling observation stems from the double-hump structure of the TEM01 mode of the pump. The key point in multiphoton complementarity is that these photons, which are prepared in an entangled state, are correlated nonlocally and can be traced mutually in both space and time.

Recent investigations showed that thermal light possesses the nonlocal spatiotemporal correlation like the entangled photons do [22,23]. Since a thermal light source is classical and macroscopic, the correlated interference and imaging with thermal light are quite different from that with entangled photons [24]. How about the complementarity principle in systems with thermal light? In fact, few investigations of complementarity concern thermal light. Cao *et al.* demonstrated complementarity between path information and interference in a thermal-light interference experiment with two symmetrically placed double-slits [25]. Nevertheless, the trajectory information, acquired by opening or closing a single slit in one arm, was completely ruined. In this paper, we show that the second-order interference and path distinguishability are complementary in a Sagnac interferometer. Different from Cao's work [25], the path information in our scheme bonds to the freedom of optical polarization. By using a Sagnac-type interferometer, we set up a double-slit apparatus which enables us to send orthogonal polarizations in the two slits. In this way, we can fetch out the trajectory information without ruining or changing the spatial distribution of each beam.

Here we investigate experimentally the interplay between path information and second-order coherence in a prototypical double-slit setup with a thermal source. A polarizing beam splitter is employed in our Sagnac-type interferometer. Also, a polarizer is used in front of the detector to postselect the which-way information of the interfered beams. By adjusting the orientation of the polarizer, we can tune the behavior of the interferometer from a complete wave-like form to a complete particle-like form.

The Sagnac-type interferometer, depicted in Fig. 1(a), is set up to examine complementarity in second-order correlation measure with thermal light. The Sagnac interferometer is composed of a polarizing beam splitter (PBS) and three mirrors (M). PBS splits thermal light into two daughter beams which are orthogonally polarized and have equal intensity. Inside the interferometer, the horizontally polarized beam, as shown by a black dashed line in Fig. 1(a), passes through the PBS and travels clockwise. The other beam, which is vertically polarized and shown by a gray line in Fig. 1(a), is reflected by the PBS and travels anticlockwise. A single slit is positioned at the midpoint of the interferometer, slightly off the optical axis. This slit allows different sections of the clockwise and anticlockwise beams pass through, resulting in an effective (equivalent) Young's double-slit interferometer as shown in Fig. 1(b).

*songxinbing@bit.edu.cn

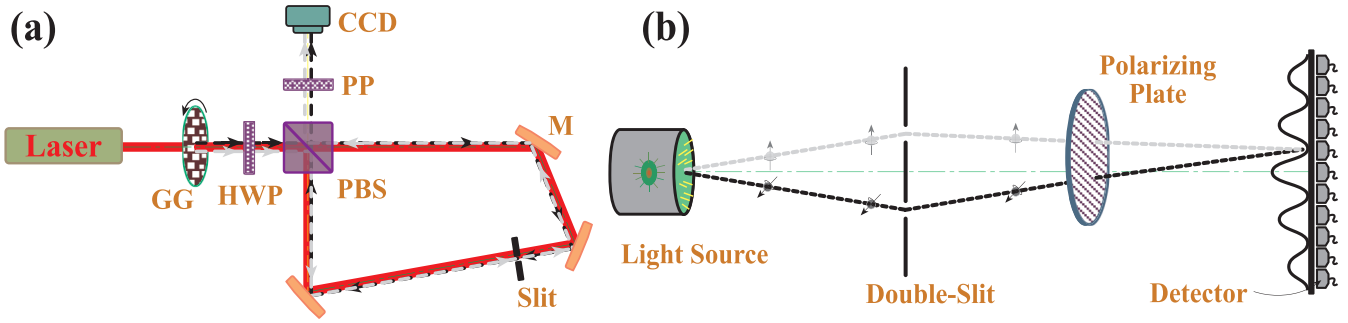

FIG. 1. Experimental setup for complementarity. (a) Experimental setup. A beam of pseudothermal light generated from the modulation of a laser beam by a GG enters a Sagnac interferometer and detected by a CCD after flowing out from the upper outport of a PBS. A slit is inserted in the interferometer with an excursion to act as a double-slit. The vertical (V) and horizontal (H) polarizing beam will pass through the slit clockwise and anticlockwise, respectively. A PP is needed before the CCD to select the polarization component to be measured. GG: ground glass; HWP: half wave plate; PBS: polarizing beam splitter; PP: polarizing plate; M: mirror. (b) Equivalent sketch of experimental setup. V and H polarizing beams from the light source pass through the up and down slits of a double-slit, and are analyzed by the detector after a polarizing plate.

Note that the two beams depicted by the black dashed and gray dashed lines are symmetric about the optical axis (shown as the dashed-dotted line) outside the interferometer. However, they are collinear inside the interferometer and pass through the slit accurately. This is because the light is reflected at odd times from the source to the detector. Also, this is the very reason why we use three mirrors in the interferometer. Therefore, our Sagnac interferometer works as a wave-front splitting interferometer. The double-slit separation is two times as much as the offset of the slit from the optical axis, and there will be no Young's fringes if the slit is placed on the optical axis.

In the experiment, the pseudothermal light source is prepared by impinging a He-Ne laser beam (wavelength $\lambda = 632.8$ nm) onto a slowly rotating ground glass (GG) with a rotation frequency of 2×10^{-3} Hz. A half wave plate (HWP) is used to preset the polarization state of the input thermal light beam. The output beam passes through a polarizing plate (PP), which selects certain polarization, and then the beam is detected by a charge-coupled device camera (CCD, MINTRON MTV-1881EX). The distances from the PBS to the GG and to the CCD are 35 and 20 cm, respectively. The perimeter of the interferometer is 66 cm. The slit width is 220 μm and its offset from the axis is 350 μm. The speckles illuminating the slit have an average size about 300 μm, which is bigger than the slit width, but smaller than the spacing of the effective double-slit.

Figure 2 depicts our experimental results. The first and second rows show the results when the polarizer PP is oriented at $\pm 45^\circ$ from the horizontal. The third row corresponds to the results when the polarizer is removed. The bottom two rows show the results when the polarizer is set at the horizontal and vertical directions, respectively. The first and second columns show the one-dimensional (1-D) and two-dimensioanl (2-D) second-order correlation results, respectively. The third column shows interference fringes obtained with coherence illumination when GG is removed. The fourth column shows a single realization of the intensity pattern at the camera for at one particular setting of the GG. Due to single-slit diffraction, the patterns in the fourth column present horizontal bright regions. The second-order correlations are calculated by averaging the information from 8000 frames intensity images, like those shown in the fourth column via $g^{(2)}(x) = \langle I(0)I(x)\rangle / \langle I(0)\rangle\langle I(x)\rangle$.

Obviously, light transmitted through the Sagnac-type interferometer carries which-way information in polarization. Indeed, as shown in the middle row of Fig. 2, the patterns contain no first-order or second-order fringes. Similarly, the two bottom rows show the results when either the H or V components are selected, thus showing just single-slit patterns. However, when the PP is oriented at $\pm 45^\circ$, we cannot distinguish the which-way information through polarization discrimination, and interference fringes appear not only in the first-order correlation but also in the second-order correlation. We address some interesting differences between the two interference patterns. The first-order interference in the two orthogonal cases of $\pm 45^\circ$ forms complementary fringes shown in Figs. 2(c) and 2(g). When the polarizer is removed, interference information is lost by adding these two patterns into a uniform, so featureless intensity is obtained and shown in Fig. 2(k). In contrast, the two second-order patterns are identical as demonstrated in Figs. 2(b) and 2(f). Both of them maximize at $x = 0$ as expected for any classical source. The complementary components, which should be added to these patterns to make them uniform are the correlations between the orthogonal components, e.g., $g^{(2)}_{+-}(x) = \langle I_+(0)I_-(x)\rangle / \langle I_+(0)\rangle\langle I_-(x)\rangle$, but they cannot be measured separately in the present setup.

We present here a simple 1-D theory to reproduce and explain the observations. We denote the transverse coordinates (normal to the slit) in the planes of double-slit and detectors by x_0 and x, respectively, and the fields in the two planes are $\mathbf{E}_0(x_0)$ and $\mathbf{E}(x)$. The distance from the double-slit to the detector is L. The output field $\mathbf{E}(x)$ can be written as [26]

$$\mathbf{E}(x) = C \int dx_0 \mathbf{E}_0(x_0) T(x_0) \exp\left[\frac{ik}{2L}(x - x_0)^2\right], \quad (1)$$

where $T(x_0)$ is the transmission function of the double-slit, k is the wave number, and C is an insignificant constant. We define $T(x_0) = T_u(x_0) + T_d(x_0)$, where T_u and T_d are the transmission of the up and down slits, which are also

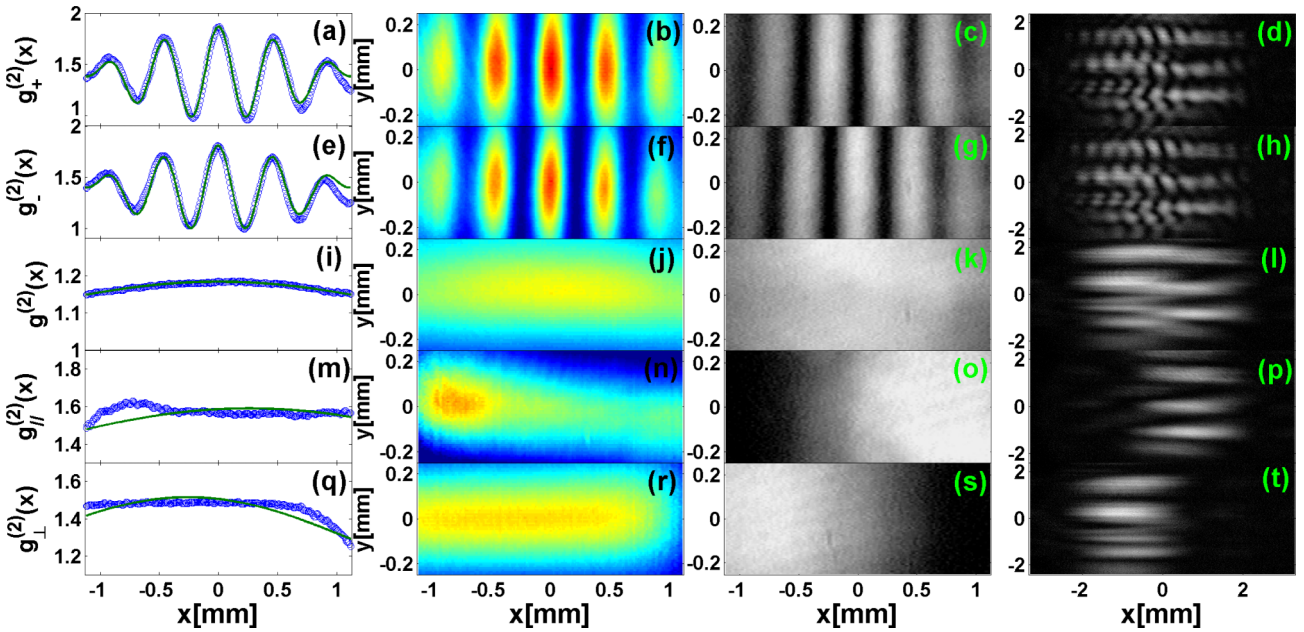

FIG. 2. Experimental results for complementarity. Rows 1 ∼ 5 correspond to the results when PP is set at ±45°, removed, at horizontal and vertical orientation, respectively. First column are the normalized second-order correlation results of 1-D, which are the cross sections of 2-D results. The open circles are experimental results and solid curves are theoretical fittings. The corresponding results of 2-D are shown in the second column. The third column demonstrate the intensity distributions for coherent light source. The speckles patterns are shown in the last column.

the transmission of the vertical and horizontal components of light, respectively. Here $T_u(x_0)$ is -1 for $(b-a)/2 < x_0 < (b+a)/2$, or 0 for other values, and $T_d(x_0)$ is 1 for $-(b+a)/2 < x_0 < -(b-a)/2$, or 0 for other values, where a and b are the slit width and spacing, respectively. The different signs are caused by the fact that one component is transmitted two times by the PSB, while the other one is reflected twice, collecting a phase shift of π. Using these notations, Eq. (1) can be written

$$\mathbf{E}(x) = \frac{C}{\sqrt{2}} \int dx_0 [\mathbf{E}_{0\perp}(x_0) T_u(x_0) + \mathbf{E}_{0\parallel}(x_0) T_d(x_0)] \times \exp\left[\frac{ik}{2L}(x-x_0)^2\right], \quad (2)$$

where $\mathbf{E}_{0\perp}$ and $\mathbf{E}_{0\parallel}$ denote the vertical and horizontal polarization fields. Further, we can decompose $\mathbf{E}_{0\perp}$ and $\mathbf{E}_{0\parallel}$ into $\mathbf{E}_{0\pm}$, that is, $\mathbf{E}_{0\perp} = [\mathbf{E}_{0+} - \mathbf{E}_{0-}]/\sqrt{2}$ and $\mathbf{E}_{0\parallel} = [\mathbf{E}_{0+} + \mathbf{E}_{0-}]/\sqrt{2}$, in which, $\mathbf{E}_{0\pm}$ represents the field for ±45° polarization, respectively. For brevity, we ignore the constant coefficient, Eq. (2) can be thus written as

$$\mathbf{E}(x) = \int dx_0 \mathbf{E}_{0+}(x_0)[T_u(x_0) + T_d(x_0)] \exp\left[\frac{ik}{2L}(x-x_0)^2\right] - \int dx_0 \mathbf{E}_{0-}(x_0)[T_u(x_0) - T_d(x_0)] \exp\left[\frac{ik}{2L}(x-x_0)^2\right]. \quad (3)$$

The normalized second-order correlation between a fixed point ($x = 0$) and the whole plane x can be described as

$$g^{(2)}(x) = \frac{\langle I(0)I(x)\rangle}{\langle I(0)\rangle\langle I(x)\rangle} = \frac{\langle \mathbf{E}^*(0)\mathbf{E}(0)\mathbf{E}^*(x)\mathbf{E}(x)\rangle}{\langle \mathbf{E}^*(0)\mathbf{E}(0)\rangle\langle \mathbf{E}^*(x)\mathbf{E}(x)\rangle}, \quad (4)$$

where $\langle\cdot\rangle$ denotes the ensemble average. We consider the light source satisfying a completely incoherent condition, i.e., $\langle \mathbf{E}_0^*(x_0)\mathbf{E}_0(x_0')\rangle = I_0\delta(x_0 - x_0')$, where I_0 is a constant with the same dimension to the light intensity. Substituting Eq. (3) into Eq. (4) and after simple but lengthy derivation, we can obtain the correlation results.

For PP set at ±45°, we mark the second correlation as $g_{\pm}^{(2)}(x)$, which is given by

$$g_{\pm}^{(2)}(x) = 1 + \frac{\left|\int dx_0 |T(x_0)| \exp\left(-ik\frac{xx_0}{L}\right)\right|^2}{\left[\int dx_0 |T(x_0)|\right]^2}. \quad (5)$$

It is easy to see that except for a constant background, there is a fringe pattern modulating the diffraction of a double-slit. The theoretical analysis matches our experimental results. However, when we have the precise knowledge of the path information, that is without the PP, the result for Eq. (4) becomes

$$g^{(2)}(x) = 1 + \frac{|\widetilde{T}_u(x)|^2 + |\widetilde{T}_d(x)|^2}{\left[\int dx_0 |T(x_0)|\right]^2}, \quad (6)$$

where $\widetilde{T}_j$ is the Fourier transformation, that $\widetilde{T}_j(x) = \int dx_0 [|T_j(x_0)|^2 \times \exp(-ik\frac{xx_0}{L})]$, where $j = u, d$. Apparently there is no interference term because which-way information erases the wave character of the light. The results for the V

and H polarizing beams are

$$g^{(2)}_{\perp,\parallel}(x) = 1 + \frac{|\widetilde{T}_{u,d}(x)|^2}{\left[\int dx_0 |T_{u,d}(x_0)|\right]^2}. \quad (7)$$

Next we discuss the intensity results when the light source is coherent, which corresponds to the case that GG is removed in the experiment. When PP is set at $\pm 45^\circ$, the corresponding intensities $I_\pm$ are

$$I_\pm(x) \propto \left| \int dx_0 [T_u(x_0) \pm T_d(x_0)] \exp\left(-ik\frac{xx_0}{L} \right) \right|^2. \quad (8)$$

The results show the expected coherent interference fringes, with a shift between them, caused by the π phase shift between the two slits when the PP shifts from $+45^\circ$ to -45°. Note the difference from the situation for second order, in which there is no change in the second-order interference as depicted in Eq. (5), which agrees with our experimental results.

When PP is set at vertical or horizontal directions, there will be single slit diffraction and no interference, that is,

$$I_{\perp,\parallel}(x) \propto \left| \int dx_0 T_{u,d}(x_0) \exp\left[-ik\frac{xx_0}{L} \right] \right|^2. \quad (9)$$

In summary, we experimentally study the incompatibility between path information and wave property in a Sagnac-type interferometer with second-order thermal light correlation. A single-slit is inserted into the interferometer to mimic Young's double-slit experiment by using two modes of the interferometer. Our results show, as expected, that the wave interference fringes can appear only when which-path information cannot be extracted and the fringes disappear otherwise. Thus, even for high-order correlation in the macroscopic case, particle and wave properties are incompatible. We hope these results may deepen the understanding of wave-particle duality for many-particle systems and also broaden the applications of Sagnac interferometers in quantum optics.

This work was supported by the National Natural Science Foundation of China (Grant Nos. 11504271 and 11304016).

[1] N. Bohr, in *Albert Einstein: Philosopher Scientist*, edited by P. A. Schilpp (Library of Living Philosophers, Evanston, IL, 1949), pp. 200–241; reprinted in *Quantum Theory and Measurement* (edited by J. A. Wheeler and W. H. Zurek (Princeton University Press, Princeton, NJ, 1983), pp. 9–49.
[2] M. O. Scully, B. G. Englert, and H. Walther, Nature **351**, 111 (1991).
[3] B. G. Englert, M. O. Scully, and H. Walther, Nature **375**, 367 (1995).
[4] E. P. Storey, S. M. Tan, M. J. Collet, and D. F. Walls, Nature **375**, 368 (1995).
[5] H. M. Wiseman, F. E. Harrison, M. J. Collett, S. M. Tan, D. F. Walls, and R. B. Killip, Phys. Rev. A **56**, 55 (1997).
[6] J.-H. Huang, S. Wölk, S.-Y. Zhu, and M. S. Zubairy, Phys. Rev. A **87**, 022107 (2013).
[7] G. S. Agarwal, J. von Zanthier, C. Skornia, and H. Walther, Phys. Rev. A **65**, 053826 (2002).
[8] G. Badurek, H. Rauch, and D. Tuppinger, Phys. Rev. A **34**, 2600 (1986).
[9] U. Eichmann, J. C. Bergquist, J. J. Bollinger, J. M. Gilligan, W. M. Itano, D. J. Wineland, and M. G. Raizen, Phys. Rev. Lett. **70**, 2359 (1993).
[10] S. Dürr, T. Nonn, and G. Rempe, Nature **395**, 33 (1998).
[11] T. J. Herzog, P. G. Kwiat, H. Weinfurter, and A. Zeilinger, Phys. Rev. Lett. **75**, 3034 (1995).
[12] E. Buks, R. Schuster, M. Heiblum, D. Mahalu, and V. Umansky, Nature **391**, 871 (1998).
[13] V. Jacques, E. Wu, F. Grosshans, F. Treussart, P. Grangier, A. Aspect, and J.-F. Roch, Phys. Rev. Lett. **100**, 220402 (2008).
[14] X. Peng, X. Zhu, D. Suter, J. Du, M. Liu, and K. Gao, Phys. Rev. A **72**, 052109 (2005).
[15] M. B. Schneider and I. A. LaPuma, Am. J. Phys. **70**, 266 (2002).
[16] J.-H. Huang, H.-Y. Liu, J.-R. Gao, M. S. Zubairy, and S.-Y. Zhu, Phys. Rev. A **88**, 013828 (2013).
[17] G. Jaeger, A. Shimony, and L. Vaidman, Phys. Rev. A **51**, 54 (1995).
[18] A. F. Abouraddy, M. B. Nasr, B. E. A. Saleh, A. V. Sergienko, and M. C. Teich, Phys. Rev. A **63**, 063803 (2001).
[19] E. Bolduc, J. Leach, F. M. Miatto, G. Leuchs, and R. W. Boyd, Proc. Natl. Acad. Sci. USA **111**, 12337 (2014).
[20] R. Menzel, D. Puhlmann, A. Heuer, and W. P. Schleich, Proc. Natl. Acad. Sci. USA. **109**, 9314 (2012).
[21] R. Menzel, A. Heuer, D. Puhlmann, K. Dechoum, M. Hillery, M. J. A. Spähn, and W. P. Schleich, J. Mod. Opt. **60**, 86 (2013).
[22] R. S. Bennink, S. J. Bentley, and R. W. Boyd, Phys. Rev. Lett. **89**, 113601 (2002).
[23] R. S. Bennink, S. J. Bentley, R. W. Boyd, and J. C. Howell, Phys. Rev. Lett. **92**, 033601 (2004).
[24] D. Z. Cao, J. Xiong, and K. Wang, Phys. Rev. A **71**, 013801 (2005).
[25] D. Z. Cao, J. Xiong, H. Tang, L. F. Lin, S. H. Zhang, and K. Wang, Phys. Rev. A **76**, 032109 (2007).
[26] J. W. Goodman, *Introduction to Fourier Optics* 2nd ed., (McGraw-Hill, New York, 1988).